Performance Analysis of DD-DPMZM based RoF link for Emerging Wireless Networks

Balram Tamrakar (balramtamrakar11@gmail.com)
KIET Group of Institution, Delhi-NCR
Krishna Singh
G. B. Pant Government Engineering College
Parvin Kumar
KIET Group of Institution, Delhi-NCR

Research Article

Keywords: Dual-Drive Dual Parallel Mach Zehnder Modulator (DD-DPMZM), Third order Intermodulation distortions (IMD3), Radio over Fiber (RoF), Spurious Free Dynamic Range (SFDR), Radio Frequency (RF)

Posted Date: June 10th, 2022

DOI: https://doi.org/10.21203/rs.3.rs-1720285/v1

Additional Declarations: No competing interests reported.

Version of Record: A version of this preprint was published at Analog Integrated Circuits and Signal Processing on January 22nd, 2024. See the published version at https://doi.org/10.1007/s10470-023-02231-2.

Abstract

This paper demonstrates the analytical approach of Linearized Radio over Fiber (RoF) link based on Dual-Drive Dual Parallel Mach Zehnder Modulator (DD-DPMZM) by properly adjusting the phase shifters and biasing of the Mach Zehnder Modulator (MZM). Two input RF tones at 7 and 8 GHz applied in the used RoF link. The proposed RoF link consists of Mach Zehnder Modulator (MZM), Parallel combination of Mach Zehnder Modulators, optical fiber and photodetector (PD). Third Order Intermodulation Distortions (IMD3) factor act as a major issue, which is responsible as performance degradation factor. Major sources of IMD3 spurious components have been investigated and suppressed in theoretical analysis before photodetection. The proposed method is designed with the help of OptSim simulation software, to confirm and validate the analytical analysis and simulation results. Analytical analysis & simulation results show that, 40 dB suppression found in IMD3 spurious components, and 30 dB $Hz^{2/3}$ enhancement found in Spurious Free Dynamic Range (SFDR), for the proposed linearized RoF link as compared to conventional MZM RoF link.

1 Introduction

Radio over Fiber (RoF) link is fulfilling the current demand of higher frequency radio spectrum [1]. The use of mm wave (30 GHz-300 GHz) with the optical fiber enables the higher frequency communication with the higher bandwidth, long distance, secure and cost-effective transmission [2]. Presently all mobile spectrum users need high speed data rates, higher bandwidth, high speed multimedia services, user friendly environment, these can be possible with the help of RoF link. RoF link also providing the large Spurious Free Dynamic Range (SFDR) and immune to Intermodulation distortions [3]. An efficient RoF link can be designed by enhancing the SFDR of the link and by suppressing all possible intermodulation distortions components. The non-linear behaviour of the used external modulator is responsible for the increment of intermodulation distortions components. For the suppressions of IMD3 spurious components and enhancement of SFDR of the RoF link, many research article have been presented in the past decades, which is based on Intensity modulator, phase-controlled modulator, dual drive modulators and dual parallel Mach Zehnder modulator (DP-MZM).

In [4] phase modulator based Analog Photonics link investigated and suppression of IMD3 demonstrated. A proper arrangement of polarizer and optical filters makes convenient to suppress approximately 25 dB IMD3 components. In [5], phase modulated, and coherent I/Q demodulation based RoF link with improved dynamic range is demonstrated. The suppression of 29 dB obtained after I/Q demodulation. In [6], Intensity Modulation based RoF link investigated. This method used advanced digital signal processing technique with proper adjustment of coherent detector to get suppression of IMD3 components approximately 26.8 dB, with some predetermined assumptions. [5] to [6] required highly calibrated coherent detector, which can increase instability of the used system. In [7], Dual Parallel MZM (DPMZM) Interferometers based single side band modulation technique analytically demonstrated and experimentally validated. In this technique 49 dB, fundamental to IMD3 ratio calculated and getting 20 dB $Hz^{2/3}$ SFDR improvement. Differential delays and other pre calibrated parameters can decay the linearization of the used RoF link. In [8], DPMZM modulator-based scheme has been proposed to get linearization in the noisy environment for large IMD3 suppression and SFDR enhancement. That research article is one of the started articles to get linearization of the RoF link using DPMZM modulator.

Various methods have been demonstrated to verify the suppression of IMD3 spurious components & to get the analytical investigation about the enhancement of SFDR [9–18]. MZM is the commonly used modulator in the RoF link and its inherent nature to exploiting the non-linear behaviour, but we are using this one due to its high stability and spectral purity. Linearization of DD-DPMZM Modulator can be achieved by proper controlling of used phase shifters and biasing of DPMZM [15–18]. The mentioned research article only providing the limited suppression of IMD3 spurious components and getting the asymmetrical splits ratios of optical power in the IMD3 spurious components compared with the fundamental component.

In the present paper a simple method to get the linearization of the RoF link in terms of suppression of large IMD3 and an enhancement of the SFDR is investigated and demonstrated. Three phase shifters of π/2 radian are used in the proposed DD-DPMZM link. Properly use of biasing voltages of DD-DPMZM gives, 40 dB suppression in IMD3 spurious components and getting 30 dB $Hz^{2/3}$ enhancement in SFDR of the proposed RoF link as compared to conventional RoF link. analytical analysis validates the simulation results in terms of the suppression of second order, third order and fifth order spurious components in the proposed expression of photodetector current. These mentioned spurious components are the major sources of IMD3.

The presented research article is organized as follows: 1. Section 1, shows the introduction and advantages of RoF link and previous works done regarding the suppression of IMD3 components and an enhancement of SFDR to get the linearized RoF link. Section 2 shows the proposed simulation model with its associated analytical analysis. Section 3 shows that the simulation work and results discussion. Section 4 shows conclusion of the proposed RoF link.

2 Principle And Operation Of Proposed Rof Link

Figure 1 shows that Simulative model of the proposed RoF Link based on DD-DPMZM. The RoF link consist of two applied RF sources, indicated as Tone-1 & Tone-2, Laser diode as a carrier source, three electrical phase shifters, a PIN photo diode, conventional MZM structure and one DD-DPMZM structure. The used Linearized RoF link consists of two MZMs, as MZM-1(Upper MZM) and MZM-2 (Lower MZM), and both modulators are represented as an intensity modulated sections and they are arranged in a parallel form to get its desired outcome. Each phase shifters have 90^0 phase shifts to get desired outcome in the suppression of IMD3 spurious components.

The Optical Intensity of the laser diode as a carrier source can be represented as:

$$E_{in}(t) = A_{LD}\exp(j\Omega_0 t)$$

1

Where Ω_0 & A_{LD} are represented as angular frequency and amplitude of the transmitted optical wave respectively. The RF source are used to generate, Two RF tones as Tone-1 & Tone-2 having frequency Ω_1 & Ω_2 respectively, with same amplitude. MZM-1 is biased with zero voltage while MZM-2 is biased at V_π voltage, here V_π is representing switching voltage.

To get the linearized modulation & large suppression of the IMD3, the RF driving voltages at four electrodes of DD-DPMZM with proper biasing can be arranged as:

$$V_{L1}(t) = V_m\left\{\cos(\Omega_1 t) + \sin(\Omega_2 \mathrm{t})\right\}$$

2

$$V_{L2}(t) = V_m\left\{\sin(\Omega_1 t) + \cos(\Omega_2 \mathrm{t})\right\}$$

3

$$V_{U1}(t) = V_m\left\{\sin(\Omega_1 t) + \sin(\Omega_2 t) + \frac{V_\pi}{2}\right\}$$

4

$$V_{U2}(t) = V_m\left\{\cos(\Omega_1 t) + \sin(\Omega_2 t) - \frac{V_\pi}{2}\right\}$$

5

Where V_m, is the amplitude of the applied RF tones. $V_{L1}(t)$ & $V_{L1}(t)$ are showing driving voltages of MZM-1 (Upper MZM); & $V_{U1}(t)$ &$V_{U2}(t)$ are showing driving voltages of MZM-2 (Lower MZM). Assume that the MZM-1 & MZM-2 have same half wave switching voltages V_π. The output of MZM-1 can be expressed as:

$$E_{MZM-1}(t) = \frac{1}{2\sqrt{2}}\alpha E_{in}(t)\left[\exp\frac{j\pi V_{L1}(t)}{V_\pi} + \exp\frac{j\pi V_{L2}(t)}{V_\pi}\right]$$

6

$$E_{MZM-1}(t) = \frac{1}{2\sqrt{2}}\alpha E_{in}(t)\left[\exp\left\{\frac{j\pi V_m}{V_\pi}[\cos\Omega_1 t + \sin\Omega_2 t]\right\} + \exp\left\{\frac{j\pi V_m}{V_\pi}[\sin\Omega_1 t + \cos\Omega_2 t]\right\}\right]$$

7

Modulation Index or Depth of Modulation is expressed as:

$$m = \frac{\pi V_m}{V_\pi}$$

8

In term of depth of modulation, the outcome of MZM-1 can be modified as:

$$E_{MZM-1}(t) = \frac{1}{2\sqrt{2}}\alpha E_{in}(t)\left[\exp\left\{jm\left[\cos\Omega_1 t + \sin\Omega_2 t\right]\right\} + \exp\left\{jm\left[\sin\Omega_1 t + \cos\Omega_2 t\right]\right\}\right]$$

9

The inner terms in the above equations assume that

$A = \exp\left(\frac{j\pi}{V_\pi}V_{L1}(t)\right)$, and $B = \exp\left(\frac{j\pi}{V_\pi}V_{L2}(t)\right)$ (10)

$A = \exp\left\{jm\left[\cos\Omega_1 t + \sin\Omega_2 t\right]\right\}$, and $\mathrm{B} = \exp\left\{jm\left[\sin\Omega_1 t + \cos\Omega_2 t\right]\right\}$ (11)

Both terms A & B can be expressed using Taylor series expansions as:

$$A = \left[1 + jm(\cos\Omega_1 t + \sin\Omega_2 t) - \frac{m^2}{2!}(\cos\Omega_1 t + \sin\Omega_2 t)^2 - \frac{jm^3}{3!}(\cos\Omega_1 t + \sin\Omega_2 t)^3 + \frac{m^4}{4!}(\cos\Omega_1 t + \sin\Omega_2 t)^4 + \frac{jm^5}{5!}(\cos\Omega_1 t + \sin\Omega_2 t)^5\right.$$

12

$$B = \left[1 + jm(\sin\Omega_1 t + \cos\Omega_2 t) - \frac{m^2}{2!}(\sin\Omega_1 t + \cos\Omega_2 t)^2 - \frac{jm^3}{3!}(\sin\Omega_1 t + \cos\Omega_2 t)^3 + \frac{m^4}{4!}(\sin\Omega_1 t + \cos\Omega_2 t)^4 + \frac{jm^5}{5!}(\sin\Omega_1 t + \cos\Omega_2 t)^5\right.$$

13

After the simplification and using Taylor series expansions in the defined terms, the outcome of MZM-1 is given as:

$$E_{MZM-1}(t) = \frac{1}{2\sqrt{2}}\alpha E_{in}(t)[A+B]$$

14

$$E_{MZM-1}(t) = \frac{1}{2\sqrt{2}}\alpha E_{in}(t)\left[\sqrt{2} + \frac{m}{2}\exp\left(\frac{j\pi}{4}\right)\{\exp j(\Omega_1 t) + \exp j(\Omega_2 t)\} + \frac{m^3}{16}\exp\left(\frac{j\pi}{4}\right)\{\exp j(2\Omega_1 - \Omega_2)t + \exp(-\Omega_1 + 2\Omega_2)t\}\right.$$

15

The outcome of the equations (15) shows that sub-MZM-1 does not originates the second order component ($\Omega_1 - \Omega_2 and \Omega_2 - \Omega_1$), which indicated that the one of the major Spurious components of IMD3 has been suppressed.

Optical output at MZM-2 is given as:

$$E_{MZM-2}(t) = \frac{1}{2\sqrt{2}}\alpha E_{in}(t)\left\{\exp\frac{j\pi V_{U1}(t)}{V_\pi} + \exp\frac{j\pi V_{U2}(t)}{V_\pi}\right\}$$

16

The inner terms in the above equations assume that

$C = \exp\left(\frac{j\pi}{V_\pi}V_{U1}(t)\right)$, and $D = \exp\left(\frac{j\pi}{V_\pi}V_{U2}(t)\right)$

$$C = \exp\frac{j\pi}{V_\pi}\left[V_m\{\sin\Omega_1 t + \sin\Omega_2 t\} + \frac{V_\pi}{2}\right]$$

17

$$D = \exp\frac{j\pi}{V_\pi}\left[V_m\{\cos\Omega_1 t + \cos\Omega_2 t\} - \frac{V_\pi}{2}\right]$$

18

Using all mentioned values of C and D in the equation number 16, then the outcome of MZM-2 is given as:

$$E_{MZM-2}(t) = \frac{1}{2\sqrt{2}}\alpha E_{in}(t)[C+D]$$

19

Using Taylor series expansions, the mentioned terms C and D, is expressed as:

$$C = j\left[1 + jm(\sin\Omega_1 t + \sin\Omega_2 t) - \frac{m^2}{2!}(\sin\Omega_1 t + \sin\Omega_2 t)^2 - \frac{jm^3}{3!}(\sin\Omega_1 t + \sin w_2 t)^3 + \frac{m^4}{4!}(\sin\Omega_1 t + \sin\Omega_2 t)^4 + \frac{jm^5}{5!}(\sin\Omega_1 t + \sin\Omega_2 t)\right.$$

20

$$D = (-j)\left[1 + jm(\cos\Omega_1 t + \cos\Omega_2 t) - \frac{m^2}{2!}(\cos\Omega_1 t + \cos\Omega_2 t)^2 - \frac{jm^3}{3!}(\cos\Omega_1 t + \cos\Omega_2 t)^3 + \frac{m^4}{4!}(\cos\Omega_1 t + \cos\Omega_2 t)^4 + \frac{jm^5}{5!}(\cos\Omega_1 t + c\right.$$

21

After the simplification and using Taylor series expansions in the defined terms, the outcome of MZM-2 is given as:

$$E_{MZM-2}(t) = \frac{1}{2\sqrt{2}}\alpha E_{in}(t)\left[\frac{m}{2}\exp\left(\frac{j\pi}{4}\right)\{\exp j(\Omega_1 t) + \exp j(\Omega_2 t)\} + \frac{m^3}{16}\exp\left(\frac{j5\pi}{4}\right)\{\exp j(2\Omega_1 - \Omega_2)t + \exp(-\Omega_1 + 2\Omega_2)t\} + \frac{m}{38}\right.$$

22

The outcome of the equations (22) shows that MZM-2 does not originates the second order component ($\Omega_1 - \Omega_2 and \Omega_2 - \Omega_1$), which indicated that the one of the major components of IMD3 has been supressed. The outcome of the equations (15) and (22) shoes that the third order component

$\{(2\Omega_1 - \Omega_2) and (-\Omega_1 + 2\Omega_2)\}$ from MZM-1 and MZM-2 respectively, having the same magnitude ($\frac{1}{2\sqrt{2}}\alpha A_{LD}\frac{m^3}{16}$), but having opposite phases. As MZM-1 having phase $\frac{\pi}{4}$, while MZM-2 having phase $\frac{5\pi}{4}$, so once they are combining at the outcome stage of the linearized RoF link, both terms are cancelled out completely. Also the outcome of the equations (15) and (22) shoes that the fifth order component $\{(3\Omega_1 - 2\Omega_2) and (-2\Omega_1 + 3\Omega_2)\}$ from MZM-1 and MZM-2 respectively, having the same magnitude ($\frac{1}{2\sqrt{2}}\alpha A_{LD}\frac{m^5}{384}$), but having opposite phases. As MZM-1 having phase $\frac{5\pi}{4}$, while MZM-2 having phase $\frac{\pi}{4}$ for the mentioned fifth order component, so once they are combining at the outcome stage of the linearized RoF link, both terms are cancelled out completely. Thus, the proposed RoF link shows that the combined outcome of the DD-DPMZM is free from the second, third and fifth order components, that one is the major resources of the IMD3.

The combined outcome of linearized RoF link is given as:

$$E_{out}(t) = [E_{MZM-1}(t) + E_{MZM-2}(t)]/2$$

After simplifications, the combined outcome of the linearized RoF link can be expressed as:

$$E_{out}(t) = \frac{1}{2\sqrt{2}}\alpha E_{in}(t)\left[1 + \frac{m}{2}\exp\left(\frac{j\pi}{4}\right)\{\exp j(\Omega_1 t) + \exp j(\Omega_2 t)\} + \frac{m^4}{64}\exp(j\pi)\{\exp j(2\Omega_1 - 2\Omega_2)t + \exp(-2\Omega_1 + 2\Omega_2)t\} + \frac{m^}{184}\right.$$

23

The equations (23) shoes that the optical outcome of linearized RoF link, it contains only the fundamental component, fourth order component & seventh order component. The fundamental component having the same magnitude $\frac{1}{\sqrt{2}}\alpha A_{LD}\frac{m}{2}$, from both sub-MZMs with the same phase $\frac{\pi}{4}$, thus the proposed RoF link enhancing the magnitude of the fundamental component, that's good indication about the linearization. The fourth and seventh order spurious components having very little magnitude as compared to the desired fundamental components, so they will impact a little effect on the proposed model performance.

Photo detector current is given as:

$$I_{PD}(t) = RE_{out}(t)E_{out}^{*}(t)$$

$$= R\frac{\alpha^2}{2}E_{in}^2(t)\left\{1 + m\sqrt{2}\left[\cos\left(\Omega_1 t + \frac{\pi}{4}\right)t + \cos\left(\Omega_2 t + \frac{\pi}{4}\right)t\right] + m^2[1 + \cos(\Omega_1 - \Omega_2)t] + \frac{m^5}{32\sqrt{2}}\left[\cos\left(-\Omega_1 t + 2\Omega_2 t - \frac{3\pi}{4}\right)t + \cos\left(\right.\right.\right.$$

24

Where R is the responsivity of PIN photodetector (PD). Eq. (24) shows the measured fundamental component with enhanced magnitude while the IMD3 spurious components $\{(2\Omega_1 - \Omega_2) and (-\Omega_1 + 2\Omega_2)\}$ having negligible magnitude compared with the fundamental components. Thus, the linearized RoF link with optimized performance can be obtained with large suppression of IMD3 spurious components in the proposed DD-DPMZM model.

From Eq. (24) the fundamental component power and IMD3 spurious component power in a simplified form is given as:

$$P_{\Omega 1} = \frac{\alpha^4 R^2 P_{LD}^2 m^2 R_{Load}}{4}$$

25

$$P_{2\Omega_1 - \Omega_2} = \frac{\alpha^4 R^2 P_{LD}^2 m^2 R_{Load}}{4 * 8^4}$$

26

Where P_{LD} is the optical power and R_{Load} is the load resistance at PIN PD. load resistance is setup to one ohm and considered attenuation coefficient is taken − 0.21 dB with permissible conditions.

3 Results Analysis And Discussion

Figure 1 is representing proposed linearized RoF link. Simulation model is set up with the help of Optical simulator (OptSim), commercial simulation software, to verify the cancellation/suppression of IMD3 spurious components. A comparison in terms of SFDR between conventional RoF link and linearized RoF link is obtained through the simulation using MATLAB software. For the performance investigation of the proposed RoF link, an optical wave via laser diode, whose center frequency is 193.414 THz with power of 16 dBm, injected to the parallel combination of MZMs (MZM-1 and MZM-2). Two RF Tones of frequency 7 GHz and 8 GHz are subjected to sub-MZMs, followed by three phase shifters. Each phase shifters have 90^0 phase shifts. Phase shifters are used such that the IMD3 Spurious components should be suppressed out completely. The transmitter bandwidth is taken 20 GHz. the conventional MZM having the same amplitude & frequency as the linearized DD-DPMZM. The excess loss and switching voltage of linearized RoF link is used at 2 dB and 5 volts respectively. the outcome of DD-DPMZM is linked with the optical fiber cable. Fiber length is considered as 5 Km for the proposed linearized RoF link, and that directly connected to the PIN PD, where detection process can be done to get the photo current and its measured electrical spectrum. Electrical spectrum of the

generated electric photo current can be easily view using electrical spectrum analyzer. The responsivity of PIN photo detector is considered as 1.0 A/W and Quantum Efficiency of PIN PD is set about to 0.799.

Figure 2 shows that the input RF tones as Tone-1 and Tone-2, centred at 7 GHz and 8 GHz, respectively. Figure 3 shows that Optical Spectrum of conventional MZM centred at 193.414 THz. Figure 4a, representing Optical Spectrum of MZM-1. Figure 4b, representing Optical Spectrum of MZM-2. Second order spurious component completely suppressed at outcome stage of MZM-1 and MZM-2, as already discussed in the analytical approach. Figure 5, representing Combined Optical Spectrum at the output of linearized RoF link. The combined output of DD-DPMZM only contain the fundamental component with enhanced magnitude, while fourth order component and seventh order component with negligible magnitude. The second order, third order and fifth order spurious component completely suppressed at the outcome stage of linearized RoF link. Figure 6 representing the Comparative Analysis of optical outcome between linearized DD-DPMZM and conventional MZM. It clearly shows that linearized DD-DPMZM structure is efficient power saving scheme than conventional MZM structure. Figure 7a, representing electrical spectrum of PIN PD used at conventional MZM. Figure 7b, representing electrical spectrum of PIN PD used at DD-DPMZM. Electrical-Signal to Intermodulation Ratio (e-SIR) for the conventional MZM is obtained 11.39 dB, while for linearized DD-DPMZM the e-SIR is about to 51 dB, thus the use of linearized RoF link provides an enhancement in e-SIR is about to 39.61 dB, which clearly means that approximately 40 dB suppression founded in IMD3 spurious components using linearized RoF link as compared with the conventional RoF link.

Figure 8a, shows that the measured SFDR of RoF link using Conventional MZM, founded as 106 dB $Hz^{2/3}$, while Fig. 8b, shows that measured SFDR for linearized DD-DPMZM, founded as 136.0 dB $Hz^{2/3}$. SFDR is enhanced by approximately 30 dB $Hz^{2/3}$, while using linearized RoF link.

Noise floor is set at -174 dBm/Hz. Figure 8 (a) and (b) shows that slope of IMD3 spurious component power changed from slope 3 to slope 5, which indicated that the major IMD3 components has been suppressed. Phase controlled based RoF link is designed, and we found that the linearity of the proposed RoF link is enhanced in a significant amount, by proper controlling the used phase shifters and biasing in DD-DPMZM structure.

Table 1
Simulation work parameters

Centre Emission Frequency of LD	**193.414 THz**
CW Power of LD	16 dBm
Linewidth of LD	0.003 MHz
Responsivity of Pin PD	1 A/W
Quantum Efficiency of PD	0.7999
-3 dB Bandwidth of PD	20 GHz
Bit Error rate	0.0227501
Q-factor	6.02 dB
Average opening of Eye	0.0246312 (a.u.)
Jitter	0.019931 ns
Sampling time	0.00418163 ns

Table 1 representing the used simulation parameters and Table 2 representing Comparison of parameters between Conventional MZM Modulator and DD-DPMZM Modulator based RoF Link. Table 2 shows that the 11.39 dB, Fundamental to IMD3 ratio has been measured for conventional MZM RoF Link, while 51.0 dB, Fundamental to IMD3 ratio has been measured for DD-DPMZM RoF Link.

Table 2
Comparison Between Conventional MZM Modulator and DD-DPMZM Modulator based RoF Link

S.No.	**Parameters**	**Conventional MZM Modulator**	**DD-DPMZM Modulator**
1	Fundamental to IMD3 Ratio	11.39 dB	51.0 dB
2	SFDR of RoF Link	106 dB $Hz^{2/3}$	136 dB $Hz^{2/3}$
2	Excess loss of MZM	2 dB	5 dB
3	Maximum Offset Voltages corresponding to phase of MZM	2.5 V	2.5 V
4	Extension Ratio Type	Ideal	Ideal
5	Voltage V_{pi}	5 V	5 V
6	Average Power Reduction due to Modulation	3.0 dB	3.0 dB
7	First Filter Notch	NA	NA
8	Chirp Factor	0.0	0.0

4 Conclusion

This research article representing linearized RoF link with large IMD3 suppression and enhancement of the SFDR using simple and adjustable electrical phase shifters. Without using any digital signal processing technique, major sources of IMD3 spurious components have been investigated and suppressed in theoretical analysis before photodetection. The proposed simulation model enhanced the linearization of the RoF link, which is in good accordance with the theoretical approach. For linearized RoF link, Fundamental to IMD3 ratio is 51 dB Measured, while for conventional RoF link, Fundamental to IMD3 ratio is 11.39 dB Measured. A suppression of 40 dB has been found in the IMD3 spurious components and enhancement of 30 dB $Hz^{2/3}$ has been found in the SFDR for linearized RoF link. For conventional RoF link measured SFDR is 106 dB $Hz^{2/3}$, while for linearized RoF link measured SFDR is 136 dB $Hz^{2/3}$. These outcomes of the proposed RoF link will be beneficial for the Emerging Wireless Networks.

Declarations

Authors Contributions BT and PK designed Simulation model and written original draft. BT and KS find the outcomes of the proposed article and made all used figures and tables. KS provides the conceptualization, formal analysis, and modelling about the research article. PK provides the supervision, conceptualization, design, analysis about the research article. All authors have read and reviewed the manuscript. The authors agree to be accountable for all aspects of the work in ensuring that queries related to the accuracy or integrity of any part of the work are appropriately investigated and resolved.

Funding There is not any type of funding for the given research article.

Data availability statement the raw materials supported to the given research article will be provided by authors, without any pre reservation, to any researcher or reviewers on reasonable request.

Declarations Authors have no competing interests as defined by Springer, or other interests that might be perceived to influence the results and/or discussion reported in the presented research article. The authors declare that the research was conducted without any commercial or financial supports that could be construed as a potential conflict of interest.

References

1. Li, X., Xiao, J., & Yu, J. (2016). Long-distance wireless mm-wave signal delivery at W-band. *Journal of Lightwave Technology*, *34*(2), 661–668
2. Zhu, M., Zhang, L., Wang, J., Cheng, L., Liu, C., & Chang, G. K. (2013). Radio-over-fiber access architecture for integrated broadband wireless services. *Journal of Lightwave Technology*, *31*(23), 3614–3620
3. Berceli, T., & Herczfeld, P. R. (2010). Microwave photonics—Historical perspective. *IEEE Transactions Microwave Theory Technology*, *58*(11), 2992–3000
4. Chen, Z., Yan, Lianshan, Guo, Yinghui, Pan, Wei, Luo, Bin, Zou, Xiahua, and Zhou, Tao. (2013). SFDR enhancement in analog photonic links by simultaneous compensation for dispersion and nonlinearity.Optics Express, 21(18),20999–21009
5. Clark, T. R., O'Connor, S. R., & Dennis, M. L. (2010). A phase-modulation I/Q-demodulation microwave-to-digital photonic link. *IEEE Transaction on Microwave Theory and Techniques*, *58*(11), 3039–3058
6. Cui, Y., Dai, Yitang, Yin, Feifei, Lv, Qiang, Li, Jianqiang, Xu, Kun, and, & Lin, J. (2014). Enhanced spurious free dynamic range in intensity modulated analog photonic link using digital post processing. IEEE Photonics Journal, 6(2)
7. Zhu, Z. H., Zhao, S. H., Tan, Q. G., & Jiang, W. (2013). A linearized optical single-sideband modulation analog microwave photonic link using dual-parallel interferometers.IEEE Photonics Journal, 5(5)
8. Korotky, S. K., & Ridder, R. M. (1990). Dual parallel modulation schemes for low-distortion analog optical transmission. *IEEE Journal on Selected Areas in Communications*, *8*(7), 1377–1381
9. Cho, T. S., & Kim, K. (2006). Effect of third-order intermodulation on radio-over-fiber systems by a dual-electrode Mach–Zehnder modulator with ODSB and OSSB signals. *Journal of Lightwave Technology*, *24*(5), 2052–2058
10. Thomas, V. A., El-Hajjar, M., & Hanzo, L. (2015). Performance improvement and cost reduction techniques for radio over fiber communication. *IEEE Communication Surveys & Tutorials*, *17*(2), 627–670
11. Paloi, F., & Haxha, S. (2018). Analysis of the carrier suppressed single sideband modulation for long distance optical communication systems. *Optik*, *161*, 230–243
12. Zheng, Z., Peng, Miao, Zhou, Hui, Chen, Ming, Jiang, Leyong, Tan, Li, Dai, Xiaoyu, and Xianga, Yuanjiang. (2018). Optical single sideband millimetre wave signal generation and transmission using 120° hybrid coupler.Optics Communications, 411,21–26
13. Tan, Q., Gao, Y., Fan, Y., & He, Y. (2018). Multi-octave analog photonic link with improved second- and third order SFDRs. *Optics Communications*, *410*, 685–689
14. Singh, S., Arya, S. K., & Singla, S. (2018). RoF system based on phase modulator employing polarization for linearization. *Journal of Optics*, *47*(4), 460–466
15. Zhu, G., Liu, W., & Fetterman, H. R. (2009). A broadband linearized coherent analog fiber- optic link employing dual parallel Mach–Zehnder modulators. *IEEE Photonics Technology Letter*, *21*(21), 1627–1629
16. Kim, S. K., Liu, W., Pie, Q., & Dalton, L. R. (2011). Nonlinear intermodulation distortion suppression in coherent analog fiber optic link using electro-optic polymeric dual parallel Mach–Zehnder modulator. *Optics Express*, *19*(8), 7865–7871
17. Liang, D., Tan, Q., Jiang, W., Zhu, Z., Li, X., & Yao, Z. (2015). Influence of power distribution on performance of intermodulation distortion suppression. *IEEE Photonics Technology Letters*, *27*(15), 16391641

18. Zhou, Y., Zhou, L., Wang, M., Xia, Y., Zhong, Y., Li, X., & Chen, J. (2016). Linearity characterization of a dual parallel silicon Mach–Zehnder modulator. *IEEE Photonics Journal*, *8*(6), 7805108

19. List of Used Tables

Figures

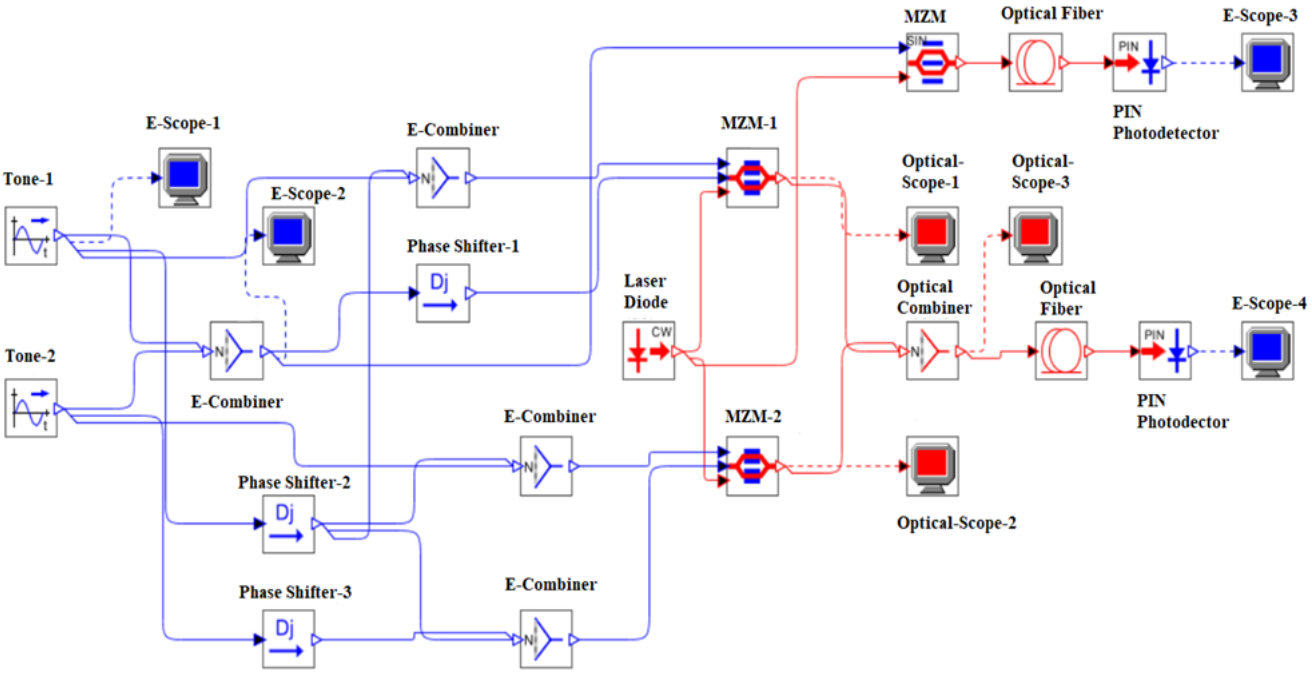

Figure 1

Simulative model of the proposed RoF Link based on DD-DPMZM.

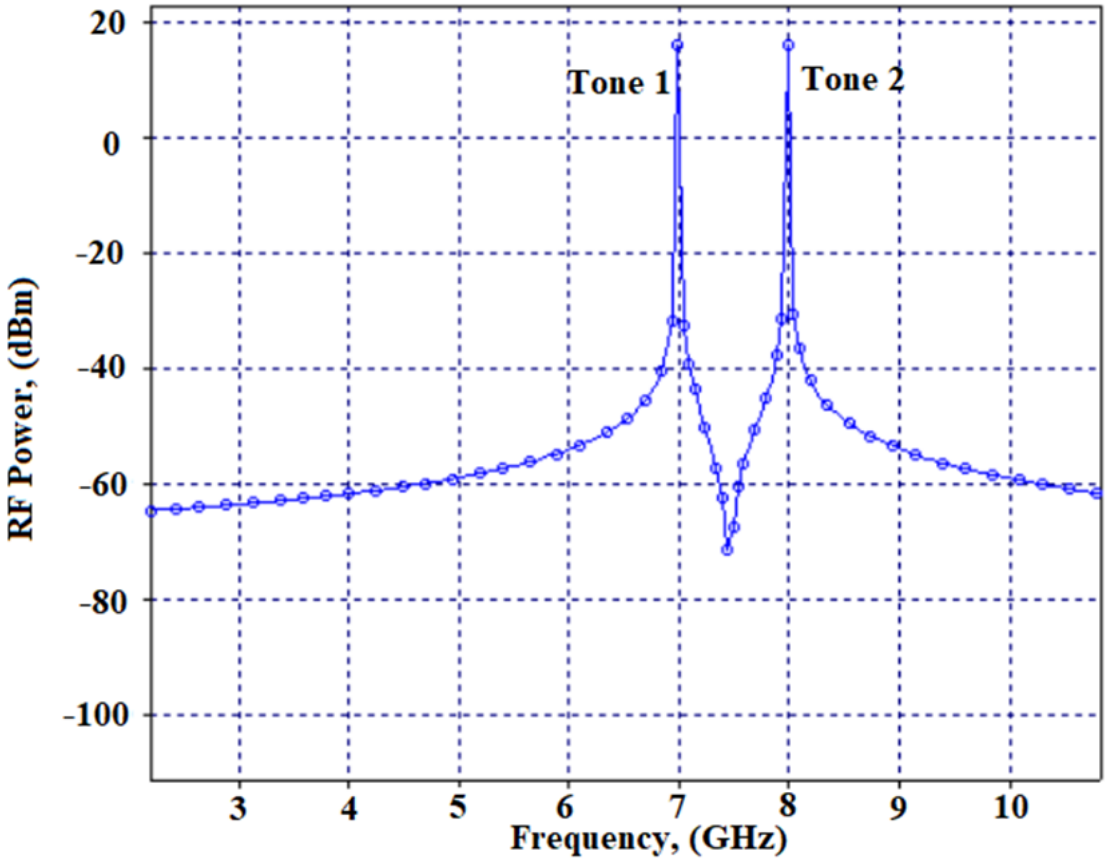

Figure 2

Input RF Tones at 7 & 8 GHz.

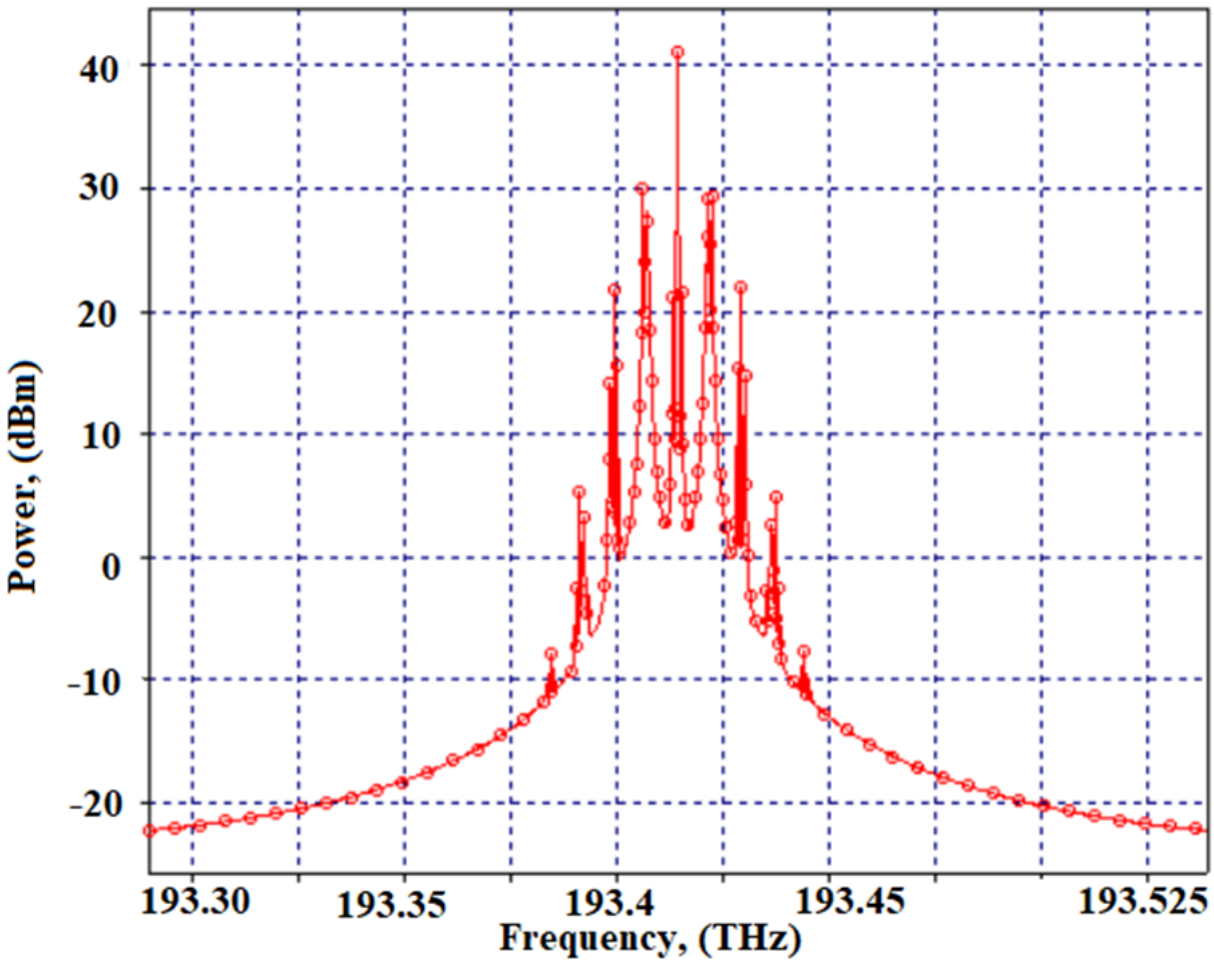

Figure 3

Optical Spectrum of conventional MZM centred at 193.414 THz.

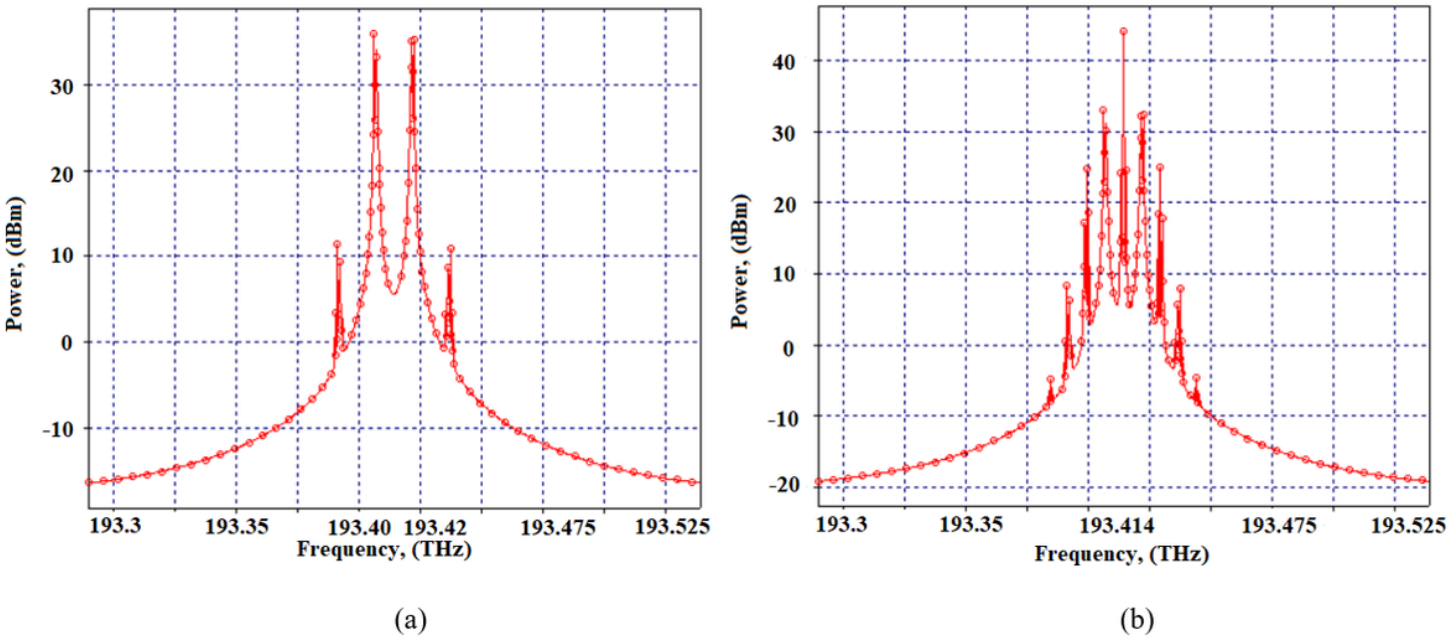

Figure 4

Optical Spectrum at the outcome stage of (a) MZM-1, (b) MZM-2

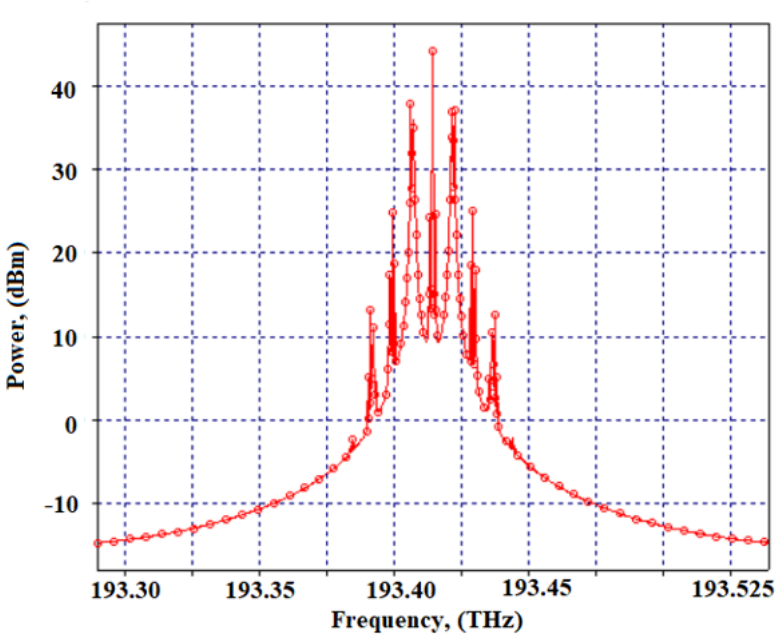

Figure 5

Combined Optical Spectrum at the outcome stage of DD-DPMZM

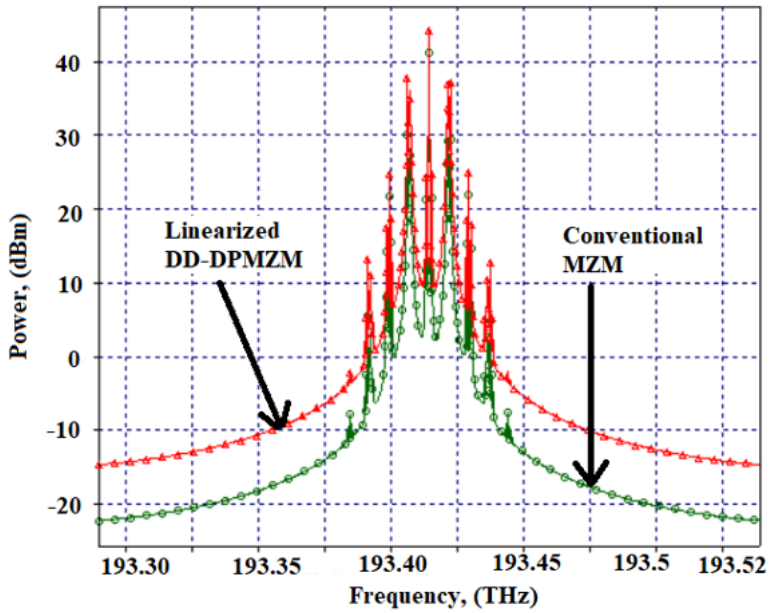

Figure 6

Comparative Analysis of optical outcome between Linearized DD-DPMZM and conventional MZM

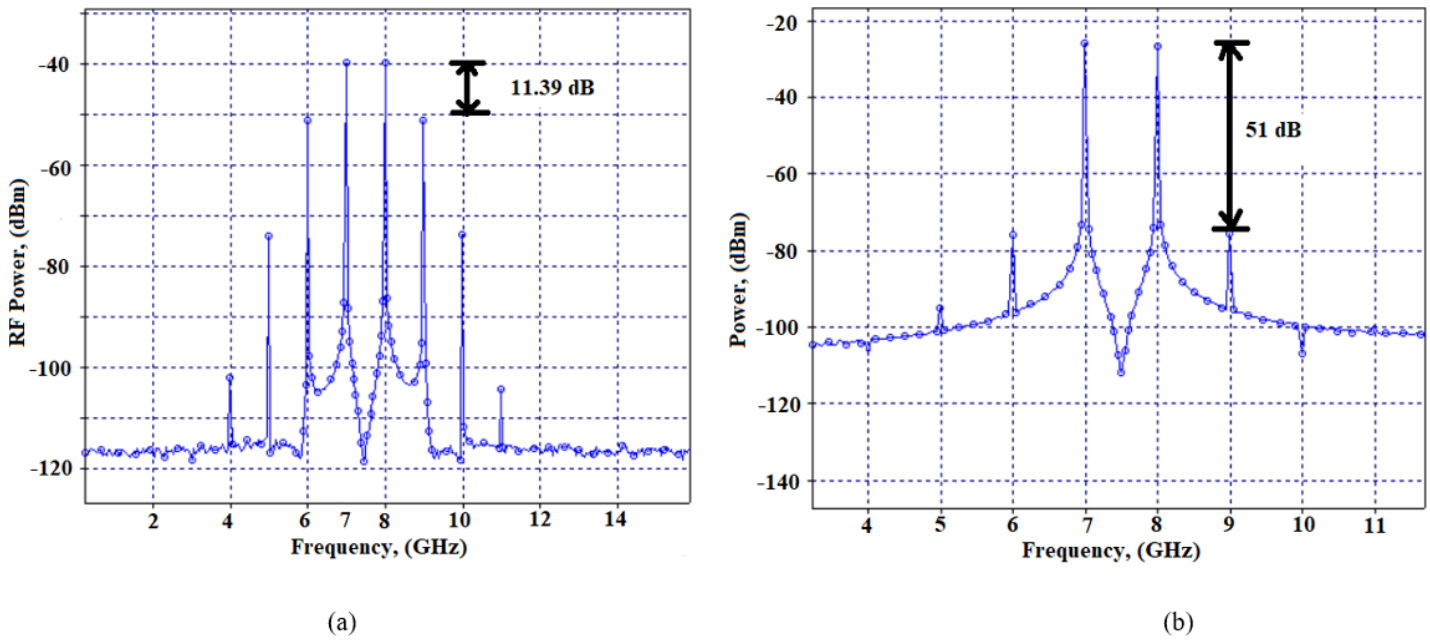

Figure 7

Electrical Spectrum at outcome stage of PIN PD for (a) conventional RoF link, (b) for Linearized RoF link.

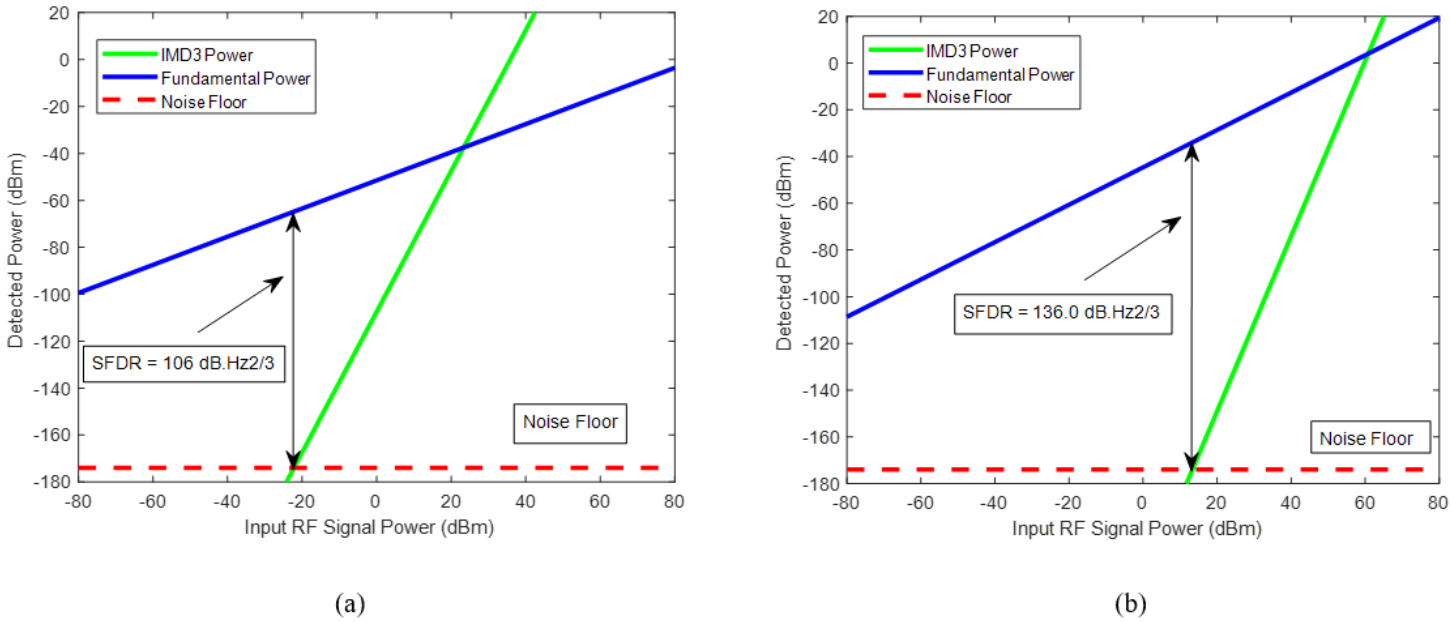

Figure 8

SFDR measurement of RoF link using (a) Conventional MZM, (b) Linearized DD-DPMZM.